

MoMa-Pos: Where Should Mobile Manipulators Stand in Cluttered Environment Before Task Execution?

Beichen Shao^{1†}, Yan Ding^{2†*}, Xingchen Wang¹, Xuefeng Xie³, Fuqiang Gu¹, Jun Luo⁴, Chao Chen^{4*}

Abstract—Mobile manipulators always need to determine feasible base positions prior to carrying out navigation-manipulation tasks. Real-world environments are often cluttered with various furniture, obstacles, and dozens of other objects. Efficiently computing base positions poses a challenge. In this work, we introduce a framework named MoMa-Pos to address this issue. MoMa-Pos first learns to predict a small set of objects that, taken together, would be sufficient for finding base positions using a graph embedding architecture. MoMa-Pos then calculates standing positions by considering furniture structures, robot models, and obstacles comprehensively. We have extensively evaluated the proposed MoMa-Pos across different settings (e.g., environment and algorithm parameters) and with various mobile manipulators. Our empirical results show that MoMa-Pos demonstrates remarkable effectiveness and efficiency in its performance, surpassing the methods in the literature. Supplementary material can be found at <https://yding25.com/MoMa-Pos>.

I. INTRODUCTION

Mobile manipulators are increasingly being used in everyday environments like homes, hospitals, and malls to perform a variety of navigation-manipulation tasks. The importance of research in this field is rapidly growing, and leading organizations, including Meta AI, have been frequently organizing mobile manipulation challenges in recent years, such as the HomeRobot [1] and Habitat Rearrangement [2] competitions. In these challenges, robots typically navigate to targets like cups or refrigerators and then perform manipulation tasks such as picking up cups or opening refrigerator doors. It is well-recognized that the success of these tasks is heavily dependent on the robots' base positioning [3]–[5]. Poor base positioning can significantly hinder the robots' ability to manipulate effectively, as illustrated in Fig. 1. Thus, identifying practical base positions is crucial for the successful completion of navigation-manipulation tasks.

However, the problem of practical base positions identification remains challenging, especially in complex environments like residential spaces. The location of the target object relative to furniture, such as refrigerators, drawers, or tables, significantly influences the robot's positioning. For instance, a robot needs to be positioned directly in front of a refrigerator to access its contents, whereas it

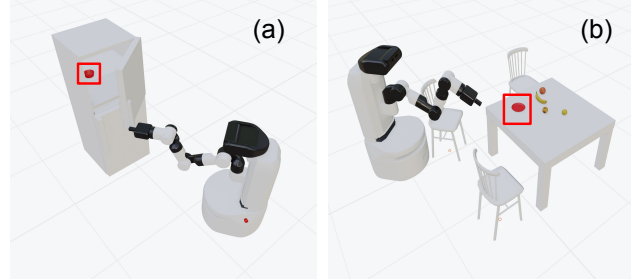


Fig. 1: The mobile manipulator's current base position is not optimal for effectively grasping the red bowl in the refrigerator (see Subfigure a) or the bowl on the dining table (see Subfigure b). This is because the robot arm's movement is hindered by a complex environment. This is because the robot arm's movement is obstructed by a complex environment.

can approach an item on a table from various angles. Such complexity is further increased by potential obstacles like chairs or children's toys near the furniture. Worse still, different robot models, each with unique design features, also require specific base positions. For example, robots with shorter arms, such as Mobile ALOHA [6] and Stretch [7], may need to position themselves closer to the target object. These varying factors add to the complexity of calculating feasible base positions.

Current solutions for determining the base positions of mobile manipulators have several limitations. One approach, detailed in [3], [8], [9], manually defines feasible base position areas but fails to consider potential obstacles near targets or differences in robot models. Another approach, as proposed in [4], employs learning-based techniques to predict feasible base positions while taking obstacles into account. Yet, this approach requires extensive data collection and model training specific to each robot and scenario, limiting its practical use. In light of these challenges, there is a critical need for a universally adaptable method. Such a method should efficiently address the complexities of various working environments and accommodate different robot models as well.

A base position is considered feasible if the robot can plan a collision-free trajectory and complete the manipulation task in the real world. This planning is typically verified in a simulation before executing it in the real world. However, simulating all environmental objects is time-consuming [10], [11]. We propose that not all objects require simulation. For example, when calculating a position to grasp a cup from a table, the robot does not need to consider distant objects, like a refrigerator. By simulating only crucial objects, we are able to reduce unnecessary modeling and collision detection.

* Corresponding authors are Yan Ding (yding25@binghamton.edu) and Chao Chen (cschaochen@cqu.edu.cn).

[†] Beichen Shao and Yan Ding contribute equally.

¹ College of Computer Science, Chongqing University

² Thomas J. Watson College of Engineering and Applied Science, Binghamton University

³ School of Management Science and Real Estate, Chongqing University

⁴ State Key Laboratory of Mechanical Transmission for Advanced Equipment, Chongqing University

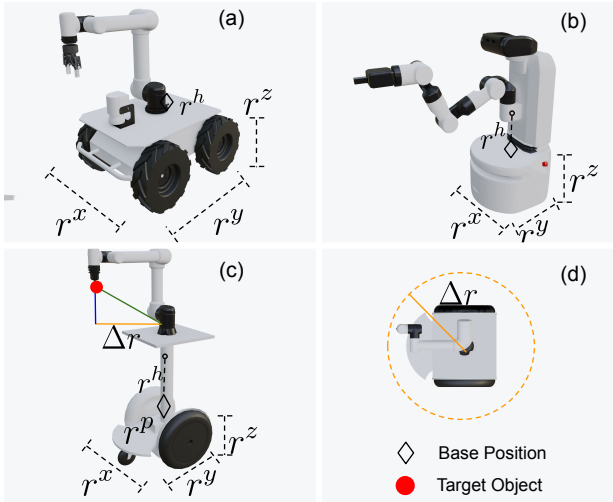


Fig. 2: A mobile manipulator model includes three primary components: a base, a body, and an arm. The symbol Δr represents the horizontal distance on the x-y plane between base’s position and the target object. For explanations of additional symbols, see Section II. There are three types of robots: Fetch, Husky+UR5e, and Segway+UR5e¹.

Nevertheless, *how to select the crucial objects is not simple*. It requires careful consideration of the specific environmental context to ensure that important objects, such as chairs near the table, are included. Failing to include sufficient items could result in incorrect assessments of feasible base positions for the robot.

This work introduces MoMa-Pos, an efficient framework for determining feasible base positions for mobile manipulators in cluttered environments before task execution. The framework begins with the selection of important objects for simulation, using a graph embedding architecture. It then dynamically identifies a potential base position area for a robot, considering its specific model, the target object’s position, and the furniture structure comprehensively. Finally, a feasible base position is determined within the area, ensuring efficiency by considering each position’s feasibility and navigation cost. MoMa-Pos has been thoroughly tested with various environments, algorithm parameters, and robots, demonstrating remarkable effectiveness and efficiency that notably outperforms existing methods in the literature.

II. PROBLEM DEFINITION

In this section, we define the *base position computation problem* in an environment, denoted as Env^O . This environment encompasses a set of objects, represented as $O = \{o_1, o_2, \dots, o_N\}$. The target object within these is specified as o_t , where $t \in [1, N]$. Each object o_i has a 3D position o_i^p , a bounding box o_i^b and a simulation model o_i^{sim} . Note that this paper presupposes the ability of current vision technologies to acquire these information, especially o_i^{sim} [12]–[14].

¹For additional information on the robots, refer to the following resources: Fetch Robotics (Zebra Technologies); Husky Unmanned Ground Vehicle (Clearpath Robotics); UR5e Collaborative Robot (Universal Robots); and Segway Robotics (Segway Robotics).

A mobile manipulator is tasked with manipulating object o_t . This robot model generally consists of at least three main components: a base, a body, and an arm, as shown in Fig. 2. These components are represented by the tuple (r^b, r^h, r^l) , where r^b indicates the base’s dimensions (r^x, r^y, r^z) - width, length, and height, respectively; r^h is the body’s height; and r^l is the arm’s extension length. The robot’s 2D base position is denoted as r^p . We assume r^p is aligned vertically with the arm base.

The primary *objective* of this work is to pinpoint a feasible base position r^{p*} for navigation-manipulation tasks. Such a position must meet two critical criteria: the arm must be able to compute collision-free trajectories for task execution, and the base must avoid collisions with any objects in Env^O .

Additionally, we define the *selective modeling problem*. In this context, the robot’s task is to select a subset of objects $S \subseteq O$ for simulation, which constitutes a subenvironment labeled Env^S . The *goal* is to compute $\min |S|$ such that $isFeasible(r^p, Env^S, Env^O)$ holds true. The function $isFeasible$ ensures that any position r^p deemed feasible in Env^S is also feasible in Env^O .

III. THE MOMA-POS FRAMEWORK

In this section, we introduce MoMa-Pos, a three-stage method targeting two key problems: predicting the importance of objects to solve *the selective modeling problem*; calculating a potential area and pinpointing a feasible base position for the mobile manipulator to address *the base position computation problem*.

A. Predicting Object Importance for Modeling

Here, our objective is to select a subset of objects, S , from the set of objects O . Instead of directly predicting S , we assess the importance of each object and include those in S , whose importance surpasses a predefined threshold α . This approach of evaluating individual object importance is efficient and allows for easy adjustment in case of initial selection errors: simply decrease α and retry, as outlined in [15]. We have developed a prediction model, $f : O \times O \rightarrow (0, 1]$, to facilitate this strategy. The model output, $f(o_i, o_t)$, indicates the likelihood of including object o_i in S relative to the target object o_t . We define this output as the *importance* of object o_i concerning object o_t .

When considering model training methods, we faced a choice between supervised and unsupervised learning techniques. Due to the difficulties in obtaining precise labels, even in small-scale environments, we chose an unsupervised learning approach. This decision was guided by our *observation that an object’s importance score, o_i , is often positively correlated with its spatial proximity to the target object, o_t , and its size, denoted as o_i^b* . Recognizing these correlations enabled us to bypass the need for exact labels, as we could infer importance based on spatial and size attributes. To implement this insight in our unsupervised model, we structured our method into three steps. The central idea is to calculate spatial proximity between objects o_i and o_t within a graph-based architecture.

1) *Modeling Environment Env^O as a Directed Graph $G = (V, E)$* : In Env^O , each object o is represented as a node $v \in V$, with attributes such as the object’s size o^b . The spatial relationships between objects are expressed through edges in the set E , where $E \subseteq V \times V$. An edge $(v_i, v_j) \in E$ signifies the spatial relationship between objects linked to nodes v_i and v_j . The *direction* of this edge reflects their spatial hierarchy. An edge $(v_i, v_j) \in E$ exists if object o_i is *on*, *in*, or *inside* object o_j , or if both objects o_i and o_j are *on the floor*. The *weight* of an edge (v_i, v_j) determined by the formula $1/\text{dist}_{xy}(o_i, o_j)$, where dist_{xy} measures the horizontal distance between o_i and o_j .

2) *Embedding Graph G with DeepWalk Algorithm*: To evaluate the importance score of object o_i (represented as node v_i in graph G), we adapted the DeepWalk algorithm, originally proposed by Perozzi et al. [16], focusing on the spatial proximity between node v_i and the target node v_t . DeepWalk generates node sequences through *random walks* on the graph. Starting at a node, it randomly moves to adjacent nodes for a set number of steps, creating a node “sentence”. These sequences, similar to sentences in natural language, help in learning nodes’ latent representations, reflecting their contextual relationships in the graph. Our approach innovates by utilizing *biased random walks*, which adjust the transition probability P between any two nodes, v_i and v_j , according to the equation below, using a weighted function $w(v_i, v_j) = k_0/\text{dist}_{xy}(o_i, o_j) + (1 - k_0) \times \text{size}(o_j)$. Here, k_0 acts as a tuning parameter. This adjustment allows for generating sequences that more accurately reflect the nodes’ significance.

$$P(v_i, v_j) = \begin{cases} \frac{w(v_i, v_j)}{\sum_{u \in N(v_i)} w(v_i, u)}, & (v_i, v_j) \in E \\ 0, & \text{otherwise} \end{cases}$$

where $N(v_i)$ represents the set of nodes adjacent to v_i .

3) *Scoring Object Importance*: After obtaining node embeddings in graph G , we determine the importance score of each object o_i (node v_i) by calculating the cosine similarity [17] with the reference target node v_t . The nodes are then ranked according to these importance scores. Objects with a score exceeding a predefined threshold α , where $\alpha \in [0.0, 1.0]$, are added to the set S . An intelligent framework should allow α to self-adjust for optimal performance. In our version, we start with a slightly higher α , based on empirical data. If MoMa-Pos fails, we reduce α to accommodate more new objects.

B. Computing Potential Base Position Area

To determine the potential base position area, A , for a robot, we consider both the robot’s model and the target object’s position, o_t^p , together. However, not every position inside A ensures successful object manipulation due to potential interference from furniture and obstacles. Our next step involves assessing each sampled position $r^p \in A$ for feasibility using a potential-based method. These two steps are detailed in the following.

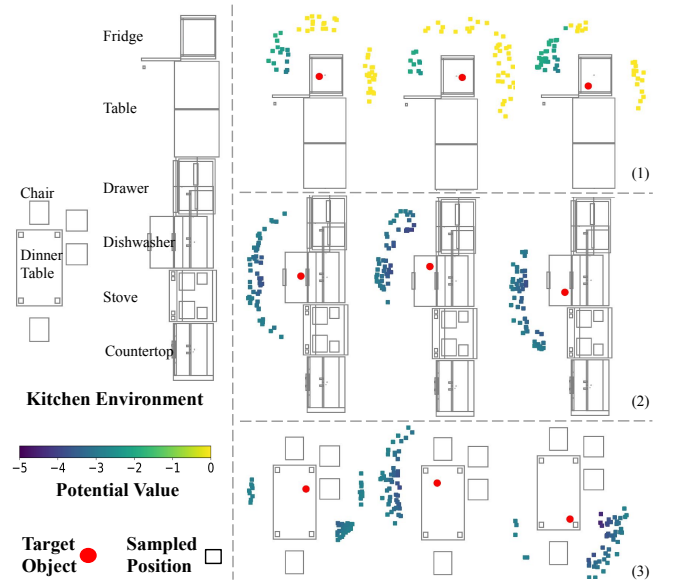


Fig. 3: The upper left figure provides a comprehensive view of the robots’ operating environment. The three figures on the right highlight selected objects crucial for the tasks at hand in simulation. The positions where the robots could potentially stand are indicated by squares. The target objects are shown with red circles, located within various pieces of furniture such as a fridge, drawer, and table. In example (1), it’s evident that when an object is positioned deep inside the fridge, the number of feasible base positions is smaller. This observation aligns with our common sense. Best viewed in the enlarged digital version.

The area A can be calculated according to the following equation:

$$A = \{r^p \mid \text{dist}_{xy}(r^p, o_t^p) \leq \Delta r, \forall i, \neg \text{overlap}(r^p, r^b, o_i^p, o_i^b)\}$$

Here, Δr is the allowable horizontal distance between a position position r^p and the target o_t^p , illustrated in a red line in Fig. 2(c). The overlap function checks collisions between the robot’s base and each surrounding object o_i by comparing their positions and boundaries. More specifically, Δr can be calculated using the formula $\sqrt{(r^l)^2 - (o_t^{p,z} - r^z - r^h)^2}$. Here, r^l , the distance from the object to the robot’s arm base (shown in green in the figure), varies within the arm’s extension range, l_1 to l_2 . These limits, l_1 and l_2 , can be derived from the robot’s DH matrix. The term $|o_t^{p,z} - r^z - r^h|$, marked as a blue line in the figure, indicates the z-axis distance between these points.

To assess the feasibility of a position $r^p \in A$, we examine it in the context of the surrounding furniture. This method is inspired by *the potential field* concept [18], where the target object o_t exerts an *attractive* force, and furniture exerts a *repulsive* force. Initially, we sample a 3D position (r^p, z) , and connect it to target object position o_t^p forming a line. We then evaluate if this line collides with the furniture’s bounding box, considering z values within the range $[\omega, r_z + r_h + l_2]$. Here, ω denotes the lowest z-axis value attainable by the robot gripper. In case of a collision, the potential value $F(r^p, z)$ is set to 0.0, indicating that the robot gripper is unable to reach the target object without encountering obstacles. Otherwise, we calculate $F(r^p, z)$ using the equation: $F(r^p, z) = k_2/\text{dist}_{xy}(r^p, o_t^p)$, where k_2

is a negative coefficient. We average the potential values for each 2D base position r^p using the formula $F(r^p) = 1/k_3 \times \sum_{i=1}^{k_3} F(r^p, z_i)$, where k_3 is a positive constant. Generally, lower potential values suggest a base position is more feasible. Fig. 3 illustrates potential values for various sampled positions in a specific kitchen environment with furniture during object manipulation tasks.

C. Identifying a Feasible Base Position

Inside the area A , we uniformly sample M 2D positions r_i^p , where $M \in [1, \infty)$ in total. Each position has an average potential value, $F(r_i^p)$, where lower values suggest better feasibility. Our MoMa-Pos aims to provide a single feasible base position. One naive approach might first try the base position with the lowest potential value and compute a collision-free trajectory to manipulate the target object using a motion planner, denoted as PLAN (e.g., RRT* [19]), to identify if the base position is feasible. If this fails, we would test positions with incrementally higher potential values until a feasible one is found. However, this method may incur high navigation costs. To optimize, our goal is to strike a balance between potential values and navigation costs.

We aim to find an optimal path that connects all sampled base positions, minimizing both factors. This problem resembles the Traveling Salesman Problem (TSP) [20], but with a key distinction: the robot does not need to return to the starting position, making it an Open TSP [21]. Considering the high number of positions (M will be pretty big), we simplify the problem by grouping positions into smaller sets based on their potential values, where each set contains T candidate positions which is much smaller than M . Each set is then analyzed to determine the optimal path, proceeding to the next set if a feasible base position is not found within the current one. Within a set, each edge directly connects two sampled positions, r_i^p and r_j^p . The weight of each edge considers both the distance $\text{dist}_{xy}(r_i^p, r_j^p)$, and their potential values. More specifically, the weight is calculated using the formula: $k_4 \times \text{dist}(r_i^p, r_j^p) + k'_4 \times (F(r_j^p) - F(r_i^p))$, where k_4 and k'_4 are two user-specified positive coefficients. To solve the Open TSP, we can apply various algorithms, ranging from exact methods [22] suitable for smaller groups (T) to heuristic [23] and metaheuristic [24] approaches for larger datasets. Upon determining the sequence of positions, we sequentially visit and compute trajectory for each. The search concludes when a collision-free trajectory is found, and the corresponding position, r^{p*} , is selected as the feasible base position for output eventually.

Lemma 1 (MoMa-Pos is complete). *Given any object importance scorer $f : O \times O \rightarrow (0, 1]$, threshold $\alpha \in [0.0, 1.0]$, and M uniformly sampled positions, $M \in [1, \infty)$, if the motion planner PLAN is complete, then MoMa-Pos is complete.*

Proof: Given the codomain of f excludes 0, an $\alpha > 0$ exists such that $\forall o \in O, f(o, o) \geq \alpha$. With $M \rightarrow \infty$, a feasible position, if existent, will be sampled eventually. Given PLAN's completeness, MoMa-Pos also achieves completeness. Hence, for any task and an infinite number

of samples, MoMa-Pos will identify at least one solution, assuming one exists, through PLAN. ■

IV. EXPERIMENTS

In our experiments, we aim to answer the following questions: **Q1:** How does MoMa-Pos's ability to identify feasible base positions compare with current approaches? **Q2:** How effective is the object importance scoring function within MoMa-Pos? **Q3:** How do key parameters within MoMa-Pos affect its performance? **Q4:** How does MoMa-Pos perform across different mobile manipulators?

A. Experimental Setup

In this study, we tasked a mobile manipulator with grasping a target object in a complex kitchen environment featuring various pieces of furniture with fixed locations, as shown in Fig. 3. Besides these pieces of furniture, there are 10 other objects, such as a plate and a bowl, placed randomly in different locations. We set one target object for the trials, with its placement varying randomly. The target positions are categorized into six types: *on the dinner table*, *on the table*, *on the countertop*, *in the fridge*, *in the drawer*, and *in the dishwasher*. These mentioned pieces of furniture can be divided into two groups: *containers* and *non-containers*. Containers, with their more complex internal structures, may increase the complexity of computing base positions. In our experiments, we ensured that the doors of these containers were fully opened. For each category, the approach for identifying base position underwent 25 trials. In each trial, the exact position of the target object was different. For instance, in one trial, the target object might be deep inside the fridge. The sampling-based motion planner employs RRT*, implemented using the well-known open-source library OMPL [25]. We chose the Segway+UR5e mobile manipulator as depicted in Fig. 2 (c), with a consistent starting position in all trials.

We compare our methods with the following baselines:

- **Habitat** [2]: For non-container furniture like tables, the closest navigable position to the target is chosen. For container furniture such as drawers and refrigerators, a fixed position relative to the furniture is selected.
- **M3** [3]: It begins by designating a specific area, divided into 5×5 cm cells. For non-container furniture, the closest navigable position to the target is chosen. For container furniture, it randomly selects base positions within the designated area until it finds one that is feasible.
- **Reuleaux** [26]: Similar to M3, it starts by designating a specific area, divided into 5×5 cm cells. It then evaluates how easily the robot can reach the target without obstacles. The robot chooses its base position randomly, prioritizing those with the highest reachability to ensure optimal accessibility.

To ensure a fair comparison, all baselines are evaluated within a complete working environment, excluding the time cost of modeling the simulation environment. We measure performance of all approaches using the following metrics:

Methods	On Dinner Table (Non-Container)			On Table (Non-Container)			On Countertop (Non-Container)		
	Time (s)	Cost (m)	Rate (%)	Time (s)	Cost (m)	Rate (%)	Time (s)	Cost (m)	Rate (%)
<i>MoMa-Pos</i> (ours)	3.5 ± 0.8	2.1 ± 0.1	100.0	3.2 ± 1.0	1.3 ± 0.0	100.0	2.4 ± 0.1	1.5 ± 0.1	100.0
<i>Habitat</i>	3.3 ± 0.4	2.2 ± 0.0	100.0	3.3 ± 1.2	1.4 ± 0.1	100.0	2.6 ± 0.1	1.7 ± 0.1	100.0
<i>M3</i>	3.3 ± 0.4	2.3 ± 0.0	100.0	3.3 ± 1.2	1.4 ± 0.0	100.0	2.8 ± 0.1	1.7 ± 0.1	100.0
<i>Reuleaux</i>	5.7 ± 1.0	2.6 ± 0.4	100.0	6.3 ± 0.6	1.9 ± 0.3	100.0	6.3 ± 0.7	2.1 ± 0.3	100.0

Methods	In Fridge (Container)			In Drawer (Container)			In Dishwasher (Container)		
	Time (s)	Cost (m)	Rate (%)	Time (s)	Cost (m)	Rate (%)	Time (s)	Cost (m)	Rate (%)
<i>MoMa-Pos</i> (ours)	15.5 ± 8.4	2.0 ± 0.3	100.0	15.8 ± 2.2	2.6 ± 0.4	100.0	12.8 ± 3.7	2.8 ± 0.3	100.0
<i>Habitat</i>	5.8 ± 2.4	1.0 ± 0.2	20.0	5.0 ± 0.1	2.1 ± 0.2	40.0	4.6 ± 1.1	1.4 ± 0.0	20.0
<i>M3</i>	50.1 ± 43.7	5.2 ± 3.1	60.0	49.5 ± 36.8	7.9 ± 5.5	60.0	50.1 ± 43.0	5.9 ± 3.9	60.0
<i>Reuleaux</i>	32.5 ± 30.8	3.3 ± 2.9	80.0	40.7 ± 10.6	5.7 ± 2.9	80.0	19.5 ± 8.2	3.0 ± 0.8	100.0

TABLE I: A comparison between MoMa-Pos and baseline methods in terms of task execution time (Time), navigation cost (Cost), and success rate (Rate) across different furniture categories, namely containers and non-containers. The optimal results are highlighted in bold.

task execution time (Time), measured in seconds; navigation cost (Cost) measured in meters; and success rate (Rate) within a 100-second timeframe. To provide a more detailed analysis of the time consumption for identifying feasible positions, we calculated the time taken for each step involved in the process. The process involves two primary stages: first, identifying potential candidates, with the time required for this phase represented by $\text{Time}_{\text{Phase1}}$; second, assessing the viability of these candidates through the application of RRT*, with the associated time consumption denoted as $\text{Time}_{\text{Phase2}}$. To concentrate on the efficiency of the task’s main elements, we omit navigation time from the task execution time. This decision stems from the robot’s moving speed variability, which can add considerable variance unrelated to the task’s completion efficiency. Instead, the navigation cost metric separately evaluates the robot’s spatial movement efficiency, ensuring it doesn’t affect the direct assessment of task performance.

Our experiments were conducted on a computer equipped with an AMD EPYC 7452 32-Core Processor, 64 CPU threads, an Nvidia GTX 2080 graphics card, and 128GB of RAM. To support reproducibility, we have made all the code publicly available. Visit our website for more information: <https://yding25.com/MoMa-Pos>.

B. Results and Analysis

1) *MoMa-Pos vs. Baselines:* We aim to answer question **Q1** here. The main results are shown in TABLE I. The table reveals that our method consistently achieves a 100% success rate across all trials in the working environment. Compared to the baseline methods (*Habitat*, *M3*, and *Reuleaux*), the success rate of MoMa-Pos is significantly higher, especially with container-type furniture like fridge. This is attributed to our method’s ability to consider furniture structure, effectively avoiding obstructions. MoMa-Pos also stands out in efficiency, outperforming baselines *M3* and *Reuleaux*. These methods depend on random sampling within a predefined area and often fail to locate a viable position quickly, leading to increased time costs and performance inconsistency, as seen with the high variance in *M3* and *Reuleaux*’s results. Although *Habitat* is more efficient sometimes, its much lower success rate, particularly with container-type furniture,

Methods	$\text{Time}_{\text{Phase1}}$	$\text{Time}_{\text{Phase2}}$
<i>MoMa-Pos</i> (ours)	0.045 ± 0.00038	3.09 ± 1.1
<i>Habitat</i>	0.097 ± 0.00049	3.19 ± 1.6

TABLE II: Time consumption comparison between MoMa-Pos and Habitat for various stages, where the target object is placed on the table.

limits its practical application. Our method not only shows significant advantages in success rate and time efficiency with container-type furniture but also ensures the lowest navigation cost for finding feasible solutions. MoMa-Pos consistently identifies a feasible solution within a maximum of 15.8 seconds in our tests.

Interestingly, MoMa-Pos exhibits slightly higher efficiency than Habitat when the target object is placed on both the table and the countertop. To understand this result, we calculated $\text{Time}_{\text{Phase1}}$ and $\text{Time}_{\text{Phase2}}$ for MoMa-Pos and Habitat in the “On Table” scenario, as shown in TABLE II. MoMa-Pos outperforms Habitat in both metrics. This is attributed to the sometimes large predefined area, which marginally increases the time needed to find a navigable position. Additionally, the time required for an IK solution near the target’s closest position is also slightly longer, likely due to increased obstacles in that area.

2) *Object Importance Prediction in MoMa-Pos:* We aim to answer question **Q2** here. Our experimentation begins by setting the threshold value α (specifically, 0.45) within the object importance prediction module. The achieved success rate of 100% confirms that no crucial object has been overlooked. Fig. 4 illustrates the task execution times for MoMa-Pos and a variant devoid of the prediction module. It is clear that incorporating prediction in MoMa-Pos markedly decreases computation time. Additionally, it is observed that the execution time for container-type furniture is slightly higher. For example, the average execution time for a fridge stands at about 4.2 seconds, in contrast to less than 1.2 seconds for a table. This variation is primarily due to the higher number of objects situated around the fridge and their inclusion within the simulation environment, consequently extending the modeling time for a fridge.

3) *Important Parameters in MoMa-Pos:* We aim to answer question **Q3** here. We evaluate the success rate of

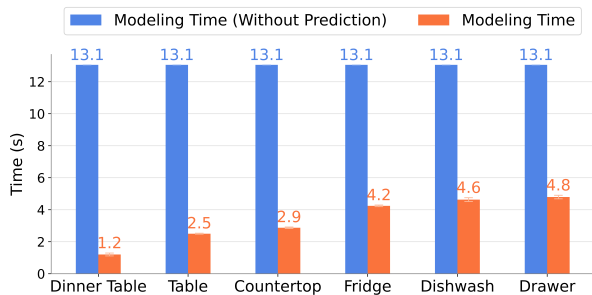


Fig. 4: The modeling time comparison between MoMa-Pos and its variant, which lacks the object importance prediction component, with the x -axis denoting the location of the target object.

MoMa-Pos over various timeframes. It’s evident that the allotted timeframe significantly influences performance metrics. Given sufficient time, MoMa-Pos is inherently complete, capable of invariably identifying a viable base position. To ascertain the impact of different time constraints on success rates, we designate timeframes of 10, 15, 20, 25, 30, and 35 seconds for our assessment. The outcomes, as detailed in TABLE III, reveal a positive correlation between extended timeframes and improved success rates, corroborating intuitive expectations. Notably, the success rate keeps 100% when the duration exceeds 20 seconds.

Timeframe (s)	10	15	20	25	30	35
Rate	86%	96%	100%	100%	100%	100%

TABLE III: Performance of MoMa-Pos across various timeframes

We are also interested in examining the distribution of time required to pinpoint a feasible base position. Fig. 5 presents the results of this examination. It is evident from the figure that the majority of the time (over 98% of the total time cost) is dedicated to identifying the feasibility through a sampling-based motion planner, namely RRT*. In contrast, the time allocated for selecting candidates is significantly lesser, accounting for less than 2% of the total time cost (approximately 0.1 seconds). This duration includes the time spent on solving the Open Traveling Salesman Problem (TSP).

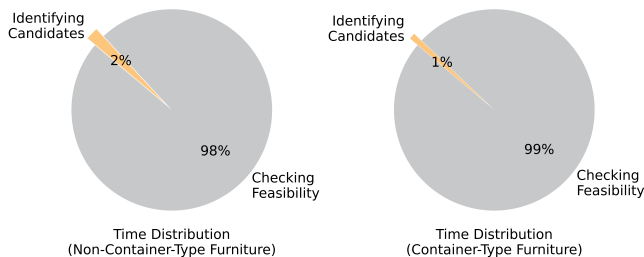


Fig. 5: Distribution of the time allocated for identifying a feasible base position when placing the target object in non-container-type and container-type furniture, respectively.

4) *Different Mobile Manipulators:* Our framework was subjected to testing across a variety of mobile manipulators.

The results, as depicted in TABLE IV, underscore a 100% success rate, highlighting the framework’s robustness. This demonstrates the versatility of our method, making it adaptable to a wide range of scenarios.

Robot Type	Fetch	Husky+UR5e	Segway+UR5e
Rate	100%	100%	100%

TABLE IV: Performance of MoMa-Pos across various robot types

V. RELATED WORK

This section discusses two principal methodologies for computing robot base positions in robotics: rule-based and learning-based approaches.

A. Rule-based Base Position Computation

Rule-based approaches typically utilize precomputed robot reachability maps to quickly determine suitable base positions. These maps, generated using Inverse Kinematics (IK) solutions, illustrate feasible tool center point (TCP) positions for a stationary robot base. Representative studies include [26]–[31]. Some techniques, such as [26], [27], use a compact 6D grid to simplify these maps, although this requires extensive grid point calculations. Frequently, identifying a single feasible base position is sufficient, rather than mapping all possible positions. Zhang et al. [5] enhanced this methodology by incorporating factors like energy efficiency and rapid execution. They combined reachability maps with evolutionary algorithms. Other strategies involve defining feasible positions manually and applying heuristic techniques for fixed-base tasks, as demonstrated in [2]. Our proposed method, MoMa-Pos, distinguishes itself in this domain by being the first to account for complex furniture structures, such as refrigerators and drawers, when determining feasible robot base positions. MoMa-Pos is not just efficient; it prioritizes identifying a single viable position, which is vital for smooth integration with other systems. Additionally, MoMa-Pos features a selective modeling process, further enhancing the system’s overall efficiency.

B. Learning-based Base Position Computation

Learning-based methods, in contrast to rule-based ones, utilize data-driven techniques for greater adaptability in various scenarios, particularly in dynamic and unstructured environments. For instance, Stulp et al. [32] directly learn the robot arm’s reachability and inverse reachability using density networks. Meanwhile, Zhang et al. [4] aim to improve the navigation of mobile manipulators in obstacle-rich environments. They develop a model, which is trained on a specialized dataset, to specifically predict the feasibility of base positions. Further, Honerkamp et al. [33] introduce a deep reinforcement learning approach for generating dynamic motions in mobile manipulators. This method effectively adapts end-effector trajectories to various kinematic scenarios and platforms, applicable in both simulations and real-world settings. Additionally, Gu et al. [3] manually define an initial base position area for robots and subsequently

train a reinforcement learning policy to execute tasks within the designated area. In contrast to these methods, our MoMa-Pos system requires significantly less training and is designed for straightforward integration with other systems. Moreover, unlike reinforcement learning-based methods, MoMa-Pos is capable of providing explicit base positions.

VI. DISCUSSION AND FUTURE WORK

In this work, we demonstrated that MoMa-Pos effectively identifies feasible positions for navigation-manipulation tasks. We conclude by acknowledging the limitations of our study, reflecting on the implications of our findings, and highlighting opportunities for future research. A significant limitation we encountered is the lack of discussion on the performance of MoMa-Pos with inaccurate simulation models. In the real world, encountering inaccurate models is common, despite the remarkable advancements in computer vision and 3D modeling technologies. We have not explored whether MoMa-Pos's performance, particularly in terms of task execution time, would deteriorate under such conditions. Theoretically, MoMa-Pos should still be able to find feasible positions, as we have demonstrated its completeness. Another constraint of the current framework is the inability of certain critical parameters, such as α , to adapt automatically. Moving forward, we aim to address these limitations to enhance MoMa-Pos's performance further.

REFERENCES

- [1] S. Yenamandra, A. Ramachandran, K. Yadav, A. Wang, M. Khanna, T. Gervet, T.-Y. Yang, V. Jain, A. W. Clegg, J. Turner, *et al.*, "Homerobot: Open-vocabulary mobile manipulation," *arXiv preprint arXiv:2306.11565*, 2023.
- [2] S. Andrew, Y. Karmesh, C. Alex, B. Vincent-Pierre, G. Aaron, C. Angel, S. Manolis, K. Zsolt, and B. Dhruv, "Habitat rearrangement challenge 2022," 2022.
- [3] J. Gu, D. S. Chaplot, H. Su, and J. Malik, "Multi-skill mobile manipulation for object rearrangement," *arXiv preprint arXiv:2209.02778*, 2022.
- [4] X. Zhang, Y. Zhu, Y. Ding, Y. Zhu, P. Stone, and S. Zhang, "Visually grounded task and motion planning for mobile manipulation," *arXiv preprint arXiv:2202.10667*, 2022.
- [5] H. Zhang, K. Mi, and Z. Zhang, "Base placement optimization for coverage mobile manipulation tasks," *arXiv preprint arXiv:2304.08246*, 2023.
- [6] Z. Fu, T. Z. Zhao, and C. Finn, "Mobile aloha: Learning bimanual mobile manipulation with low-cost whole-body teleoperation," in *arXiv*, 2024.
- [7] C. C. Kemp, A. Edsinger, H. M. Clever, and B. Matulevich, "The design of stretch: A compact, lightweight mobile manipulator for indoor human environments," in *International Conference on Robotics and Automation (ICRA)*, 2022, pp. 3150–3157.
- [8] A. Szot, A. Clegg, E. Undersander, E. Wijmans, Y. Zhao, J. Turner, N. Maestre, M. Mukadam, D. S. Chaplot, O. Maksymets, *et al.*, "Habitat 2.0: Training home assistants to rearrange their habitat," *Advances in Neural Information Processing Systems*, vol. 34, pp. 251–266, 2021.
- [9] X. Puig, E. Undersander, A. Szot, M. D. Cote, T.-Y. Yang, R. Partsey, R. Desai, A. W. Clegg, M. Hlavac, S. Y. Min, *et al.*, "Habitat 3.0: A co-habitat for humans, avatars and robots," *arXiv preprint arXiv:2310.13724*, 2023.
- [10] K. Mo, S. Zhu, A. X. Chang, L. Yi, S. Tripathi, L. J. Guibas, and H. Su, "Partnet: A large-scale benchmark for fine-grained and hierarchical part-level 3d object understanding," in *IEEE/CVF conference on Computer Vision and Pattern Recognition*, 2019, pp. 909–918.
- [11] Q. Chen, M. Memmel, A. Fang, A. Walsman, D. Fox, and A. Gupta, "Urdformer: Constructing interactive realistic scenes from real images via simulation and generative modeling," in *Towards Generalist Robots: Learning Paradigms for Scalable Skill Acquisition@CoRL2023*, 2023.
- [12] W. Liu, D. Anguelov, D. Erhan, C. Szegedy, S. Reed, C.-Y. Fu, and A. C. Berg, "Ssd: Single shot multibox detector," in *ECCV*, 2016, pp. 21–37.
- [13] R. Girshick, "Fast R-CNN," in *ICCV*, 2015, pp. 1440–1448.
- [14] T. Hodaň, M. Sundermeyer, B. Drost, Y. Labbé, E. Brachmann, F. Michel, C. Rother, and J. Matas, "Bop challenge 2020 on 6d object localization," in *ECCV Workshops*, 2020, pp. 577–594.
- [15] T. Silver, R. Chitnis, A. Curtis, J. B. Tenenbaum, T. Lozano-Perez, and L. P. Kaelbling, "Planning with learned object importance in large problem instances using graph neural networks," in *AAAI*, vol. 35, no. 13, 2021, pp. 11 962–11 971.
- [16] B. Perozzi, R. Al-Rfou, and S. Skiena, "Deepwalk: Online learning of social representations," in *Proceedings of the 20th ACM SIGKDD International Conference on Knowledge Discovery and Data Mining*, 2014, pp. 701–710.
- [17] M. Vijaymeena and K. Kavitha, "A survey on similarity measures in text mining," *Machine Learning and Applications: An International Journal*, vol. 3, no. 2, pp. 19–28, 2016.
- [18] S. S. Ge and Y. J. Cui, "Dynamic motion planning for mobile robots using potential field method," *Autonomous robots*, vol. 13, pp. 207–222, 2002.
- [19] S. Karaman and E. Frazzoli, "Sampling-based algorithms for optimal motion planning," *The international journal of robotics research*, vol. 30, no. 7, pp. 846–894, 2011.
- [20] K. L. Hoffman, M. Padberg, G. Rinaldi, *et al.*, "Traveling salesman problem," *Encyclopedia of operations research and management science*, vol. 1, pp. 1573–1578, 2013.
- [21] H. H. Chieng and N. Wahid, "A performance comparison of genetic algorithm's mutation operators in n-cities open loop travelling salesman problem," in *Recent Advances on Soft Computing and Data Mining: SCDM-2014*. Springer, 2014, pp. 89–97.
- [22] S. Boyd and J. Mattingley, "Branch and bound methods," *Notes for EE364b, Stanford University*, vol. 2006, p. 07, 2007.
- [23] G. Kizilates and F. Nuriyeva, "On the nearest neighbor algorithms for the traveling salesman problem," in *Advances in Computational Science, Engineering and Information Technology: CCSEIT-2013*. Springer, 2013, pp. 111–118.
- [24] E. Osaba, X.-S. Yang, and J. Del Ser, "Traveling salesman problem: a perspective review of recent research and new results with bio-inspired metaheuristics," *Nature-inspired Computation and Swarm Intelligence*, pp. 135–164, 2020.
- [25] I. A. Sucan, M. Moll, and L. E. Kavraki, "The open motion planning library," *IEEE Robotics & Automation Magazine*, vol. 19, no. 4, pp. 72–82, 2012.
- [26] A. Makhmal and A. K. Goins, "Reuleaux: Robot base placement by reachability analysis," in *IEEE International Conference on Robotic Computing (IRC)*, 2018, pp. 137–142.
- [27] N. Vahrenkamp, T. Asfour, and R. Dillmann, "Robot placement based on reachability inversion," in *IEEE International Conference on Robotics and Automation*, 2013, pp. 1970–1975.
- [28] F. Zacharias, C. Borst, M. Beetz, and G. Hirzinger, "Positioning mobile manipulators to perform constrained linear trajectories," in *IROS*, 2008, pp. 2578–2584.
- [29] M. Attamimi, K. Ito, T. Nakamura, and T. Nagai, "A planning method for efficient mobile manipulation considering ambiguity," in *IEEE/RSJ International Conference on Intelligent Robots and Systems*, 2012, pp. 965–972.
- [30] F. Zacharias, C. Borst, and G. Hirzinger, "Capturing robot workspace structure: representing robot capabilities," in *IROS*, 2007, pp. 3229–3236.
- [31] F. Reister, M. Grotz, and T. Asfour, "Combining navigation and manipulation costs for time-efficient robot placement in mobile manipulation tasks," *IEEE Robotics and Automation Letters*, vol. 7, no. 4, pp. 9913–9920, 2022.
- [32] F. Stulp, A. Fedrizzi, and M. Beetz, "Action-related place-based mobile manipulation," in *IROS*, 2009, pp. 3115–3120.
- [33] D. Honerkamp, T. Welschehold, and A. Valada, "Learning kinematic feasibility for mobile manipulation through deep reinforcement learning," *IEEE Robotics and Automation Letters*, vol. 6, no. 4, pp. 6289–6296, 2021.